
This is an electronic reprint of the original article.
This reprint may differ from the original in pagination and typographic detail.

Schulz, S.; Tanner, D. S. P.; O'Reilly, E. P.; Caro, M. A.; Tang, F.; Griffiths, J. T.; Oehler, F.; Kappers, M.J.; Oliver, R.A.; Humphreys, C.J.; Sutherland, D.; Davies, M.J.; Dawson, P.

Theoretical and experimental analysis of the photoluminescence and photoluminescence excitation spectroscopy spectra of m-plane InGaN/GaN quantum wells

Published in:
Applied Physics Letters

DOI:
[10.1063/1.4968591](https://doi.org/10.1063/1.4968591)

Published: 28/11/2016

Document Version
Publisher's PDF, also known as Version of record

Please cite the original version:
Schulz, S., Tanner, D. S. P., O'Reilly, E. P., Caro, M. A., Tang, F., Griffiths, J. T., Oehler, F., Kappers, M. J., Oliver, R. A., Humphreys, C. J., Sutherland, D., Davies, M. J., & Dawson, P. (2016). Theoretical and experimental analysis of the photoluminescence and photoluminescence excitation spectroscopy spectra of m-plane InGaN/GaN quantum wells. *Applied Physics Letters*, 109(22), Article 223102.
<https://doi.org/10.1063/1.4968591>

This material is protected by copyright and other intellectual property rights, and duplication or sale of all or part of any of the repository collections is not permitted, except that material may be duplicated by you for your research use or educational purposes in electronic or print form. You must obtain permission for any other use. Electronic or print copies may not be offered, whether for sale or otherwise to anyone who is not an authorised user.

Theoretical and experimental analysis of the photoluminescence and photoluminescence excitation spectroscopy spectra of m-plane InGaN/GaN quantum wells

S. Schulz, D. S. P. Tanner, E. P. O'Reilly, M. A. Caro, F. Tang, J. T. Griffiths, F. Oehler, M. J. Kappers, R. A. Oliver, C. J. Humphreys, D. Sutherland, M. J. Davies, and P. Dawson

Citation: *Appl. Phys. Lett.* **109**, 223102 (2016); doi: 10.1063/1.4968591

View online: <https://doi.org/10.1063/1.4968591>

View Table of Contents: <http://aip.scitation.org/toc/apl/109/22>

Published by the [American Institute of Physics](#)

Articles you may be interested in

[Carrier localization in the vicinity of dislocations in InGaN](#)

Journal of Applied Physics **121**, 013104 (2017); 10.1063/1.4973278

[Radiative recombination mechanisms in polar and non-polar InGaN/GaN quantum well LED structures](#)

Applied Physics Letters **109**, 151110 (2016); 10.1063/1.4964842

[Local carrier recombination and associated dynamics in m-plane InGaN/GaN quantum wells probed by picosecond cathodoluminescence](#)

Applied Physics Letters **109**, 232103 (2016); 10.1063/1.4971366

[The nature of carrier localisation in polar and nonpolar InGaN/GaN quantum wells](#)

Journal of Applied Physics **119**, 181505 (2016); 10.1063/1.4948237

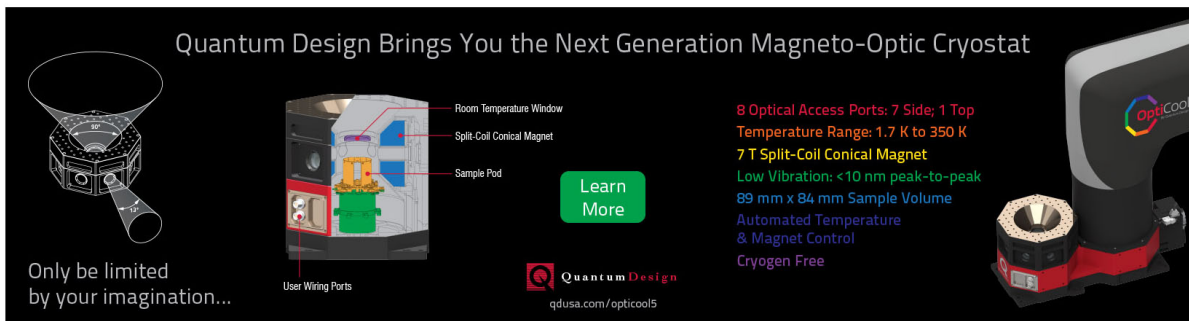
[Temperature-dependent recombination coefficients in InGaN light-emitting diodes: Hole localization, Auger processes, and the green gap](#)

Applied Physics Letters **109**, 161103 (2016); 10.1063/1.4965298

[Auger recombination in InGaN measured by photoluminescence](#)

Applied Physics Letters **91**, 141101 (2007); 10.1063/1.2785135

Quantum Design Brings You the Next Generation Magneto-Optic Cryostat



Only be limited by your imagination...

Learn More

Quantum Design
qdusa.com/opticool5

8 Optical Access Ports: 7 Side; 1 Top
Temperature Range: 1.7 K to 350 K
7 T Split-Coil Conical Magnet
Low Vibration: <10 nm peak-to-peak
89 mm x 84 mm Sample Volume
Automated Temperature & Magnet Control
Cryogen Free

Theoretical and experimental analysis of the photoluminescence and photoluminescence excitation spectroscopy spectra of *m*-plane InGaN/GaN quantum wells

S. Schulz,¹ D. S. P. Tanner,^{1,2} E. P. O'Reilly,^{1,2} M. A. Caro,^{3,4} F. Tang,⁵ J. T. Griffiths,⁵ F. Oehler,⁵ M. J. Kappers,⁵ R. A. Oliver,⁵ C. J. Humphreys,⁵ D. Sutherland,⁶ M. J. Davies,⁶ and P. Dawson⁶

¹Photonics Theory Group, Tyndall National Institute, Dyke Parade, Cork, Ireland

²Department of Physics, University College Cork, Cork, Ireland

³Department of Electrical Engineering and Automation, Aalto University, Espoo 02150, Finland

⁴COMP Centre of Excellence in Computational Nanoscience, Aalto University, Espoo 02150, Finland

⁵Department of Materials Science and Metallurgy, University of Cambridge, Cambridge CB3 0FS, United Kingdom

⁶School of Physics and Astronomy, Photon Science Institute, University of Manchester, Manchester M13 9PL, United Kingdom

(Received 23 September 2016; accepted 5 November 2016; published online 28 November 2016)

We present a combined theoretical and experimental analysis of the optical properties of *m*-plane InGaN/GaN quantum wells. The sample was studied by photoluminescence and photoluminescence excitation spectroscopy at low temperature. The spectra show a large Stokes shift between the lowest exciton peak in the excitation spectra and the peak of the photoluminescence spectrum. This behavior is indicative of strong carrier localization effects. These experimental results are complemented by tight-binding calculations, accounting for random alloy fluctuations and Coulomb effects. The theoretical data explain the main features of the experimental spectra. Moreover, by comparison with calculations based on a virtual crystal approximation, the importance of carrier localization effects due to random alloy fluctuations is explicitly shown. *Published by AIP Publishing.*

[<http://dx.doi.org/10.1063/1.4968591>]

Quantum well (QW) structures based on InGaN alloys form the cornerstone of modern blue light emitting devices.¹ Despite the immense success of InGaN-based systems, we are just beginning to understand their fundamental properties and the impact they have on device performance.^{2,3} For instance, in comparison with heterostructures based on other III–V alloys, e.g., InGaAs, the defect densities in InGaN/GaN QWs are very high.^{4,5} Given this fact, it is surprising that these systems are useful for optoelectronic devices. The defect insensitivity of InGaN-based systems has been attributed to carrier localization effects, which prevent the diffusion of carriers to non-radiative recombination centres.⁶ Experimentally, clear indications of the presence of localized states have been given. For instance, the “S-shape” temperature dependence of the photoluminescence (PL) peak energies presents such an experimental indication.^{7,8} Quite often the quantity known as the Stokes shift (SS) is mentioned as being further evidence of carrier localization. As originally described in GaAs QWs, the SS was the energy difference between the peak of the lowest lying exciton transition in absorption or photoluminescence excitation spectroscopy (PLE) and the peak of the PL spectrum at low temperatures.^{9,10} For GaAs and InGaAs QWs, the SS is typically only a few meV and is caused by the exciton localization at interface states. It should be noted that in these measurements the SS is precisely defined, being the energy difference between two peaks in the respective spectra. Turning to polar InGaN QWs, the SSs are much larger and values around 150 meV are often quoted.¹¹ It is important to note that the definition of the energy with respect to which the PL

peak is shifted is somewhat arbitrary. This is because PLE or absorption spectra from polar InGaN QWs do not exhibit any well-defined exciton peaks. This is largely due to the combined effects of built-in fields and inhomogeneous broadening.¹² In an ideal QW, there should be no SS as long as the dominant emission is excitonic; thus, absorption and emission peaks will have the same energy. In a disordered system with localized states, one expects a higher density of states (DOS) for the continuum states compared with the density of lower energy localized states. Thus, the high density of continuum states will dominate the absorption process, while at low temperature the emission is dominated by recombination involving carriers trapped at the energetically lowest states which, in a system where disorder effects are dominant, are the localized states. To shed more light on localization effects in InGaN QWs and to investigate quantitatively their relation to the SS, the combination of PL and PLE spectroscopy on *non-polar* InGaN QWs presents a promising system, since these systems should ideally be field-free.¹³ Indeed, as we have reported previously, non-polar InGaN/GaN *a*- and *m*-plane¹⁴ and GaN/AlGaIn *a*-plane¹⁵ QWs all show well resolved exciton peaks in low temperature PLE spectroscopy. This allows for a well-defined measurement of any SS.

From a theoretical perspective, the study of emission and absorption properties of a highly disordered system is challenging. First, only very recently theoretical studies have accounted for localization effects due to the disorder in realistic wurtzite InGaN QWs.^{2,14,16–18} The theoretical approaches range from modified continuum-based studies up

to atomistic calculations. All these studies clearly show that alloy fluctuations in wurtzite InGaN/GaN QWs lead to strong carrier localization effects. These investigations have mainly addressed a few energetically low-lying states which are relevant to describe PL spectra. For the analysis of PLE or absorption spectra the full DOS, including localized states, is of central importance to explain the SS. A further complication is added to the modeling process when studying *non-polar* InGaN QWs. In contrast to *c*-plane systems, where the strong built-in fields dominate the optical properties of these structures, these fields are ideally absent in non-polar wells. This has far reaching consequences since Coulomb effects become important for a detailed understanding of the optical properties.⁵ Thus, the challenge for the theoretical modeling of PL and PLE spectra is not only that a large number of electron and hole (localized) states have to be considered but also the Coulomb interaction between carriers in these states.

In this paper, we present such a theoretical study. Our model is based on an atomistic tight-binding (TB) model, taking local strain and built-in potential fluctuations due to (random) alloy fluctuations into account.^{14,17,19} With this model, we have addressed the PL and PLE spectrum of a non-polar *m*-plane InGaN/GaN QW that has been experimentally characterized by a variety of different methods.¹⁴ Equipped with this knowledge about the structural features, more than 100 hole and 20 electron single-particle states have been calculated. Coulomb effects have been accounted for by performing a configuration interaction (CI) calculation. This allowed us to obtain emission and absorption spectra. These calculations have been compared to results from (i) a virtual crystal approximation (VCA) of the system, which neglects the effect of alloy disorder completely, and (ii) low temperature PL and PLE studies. The combination of PL and PLE measurements reveals a significant SS (180 meV), while the VCA does not predict such a shift. This originates from the fact that the VCA neglects the effect of random alloy fluctuations. However, the VCA explains the main features of the PLE spectrum (e.g., splitting of excitonic states). These features are also captured by the fully atomistic treatment. Moreover, a discernible SS is observed when a random alloy distribution is assumed in the QW. Furthermore, random alloy fluctuations result in a significant broadening of the PL and PLE spectra, similar to the experiment. Thus, our combined theoretical and experimental study reveals that random alloy fluctuations significantly contribute to the SS experimentally observed in *m*-plane InGaN QWs.

The *m*-plane InGaN/GaN multi-QW (MQW) sample studied here has been grown on a free-standing *m*-plane (1–100) GaN substrate by metal organic vapor phase epitaxy. The substrate had a misorientation of $2^\circ \pm 0.2^\circ$ in the negative *c*-direction. More information about growth and defect densities can be found in Ref. 14.

To obtain a detailed picture of the structural properties of the sample, a variety of different experimental approaches have been applied. The In content, well and barrier width have been determined by x-ray diffraction (XRD) measurements, revealing a well width of 2.0 ± 0.3 nm and an In content of $18.3 \pm 0.7\%$. Additionally, the In content of the sample was determined by atom probe tomography (APT), resulting in a value of $17.0 \pm 0.6\%$. The APT analysis has

also been used to gain insight into the In distribution in the well. This study revealed that a random distribution of the In atoms in the active region of the sample is a reasonable initial assumption but subtle deviations from randomness cannot be ruled out.¹⁴

The sample was further characterized experimentally by PL and polarized PLE (P-PLE) spectroscopy. These measurements were carried out either applying excitation from a CW He/Cd laser or by using a 300 W xenon lamp and a monochromator producing a tunable or fixed excitation source. A 0.85 m double-grating spectrometer and a Peltier cooled GaAs photomultiplier with standard lock-in detection techniques have been used to obtain the spectra. More details are given in Ref. 14.

The results of the low temperature PL and PLE study are shown in Fig. 1(a). The black solid line corresponds to the (unpolarized) PL spectrum, while the P-PLE spectra are shown by (blue) dashed and (red) dashed-dotted lines. In the case of the blue dashed line, the plane of polarization of the incident light is perpendicular to the *c*-axis of the crystal ($\mathbf{E} \perp \mathbf{c}$). The red dashed-dotted line depicts the result for $\mathbf{E} \parallel \mathbf{c}$. Several features of the spectra are of interest for the present study. First, we observe that the PL spectrum is very broad with a full width at half maximum (FWHM) of 135 meV. Second, in the PLE spectra we observe distinct peaks that are attributable to the creation of free excitons. We find a splitting of $\Delta E_{1,\text{exp}}^{\perp,\parallel} \approx 35$ meV of the two lowest energy exciton peaks for both light polarization directions, denoted by $E_{1,\text{exp}}^{\perp}$ and $E_{1,\text{exp}}^{\parallel}$, respectively (cf. Fig. 1(a)). This splitting can be attributed to the fact that the confinement along the growth direction breaks the degeneracy of the two topmost valence bands in a wurtzite crystal, leaving us with the situation that the topmost valence state is oriented perpendicular to the growth direction and perpendicular to the *c*-axis.¹⁵ Assuming growth along the *y*-direction, this state is $|X\rangle$ -like in character. Due to the positive crystal field splitting energy in InN and GaN, the $|Z\rangle$ -like state, which is parallel to the *c*-axis and detectable in $\mathbf{E} \parallel \mathbf{c}$ configuration, lies energetically slightly below the $|X\rangle$ -like state. On the high energy side of the P-PLE spectrum, we find a second set of these peaks ($E_{2,\text{exp}}^{\perp}$ and $E_{2,\text{exp}}^{\parallel}$), which can be attributed to transitions between higher lying electron and hole states. The peak of the PL spectrum lies 180 meV (the SS) below the energy of the lowest lying free exciton transition in the P-PLE spectra. This occurs because before the excitons decay either by radiative or non-radiative processes they can relax and be localized at local potential minima in the QWs. Thus, carrier localization plays an important role in the optical properties of these systems.

We address this system now from a theoretical point of view. To do so, the calculations have been carried out in the framework of an atomistic TB model combined with a local polarization theory. Details of the model and how it treats random alloy effects can be found in Refs. 17 and 19. However, before turning to the fully atomistic calculation, we have performed a VCA calculation. This means that we are using a linear interpolation of all required input parameters, e.g., elastic constants, but allowing for a band gap bowing parameter of approximately 1.4 eV. It is important to stress here that this calculation is presented simply as a

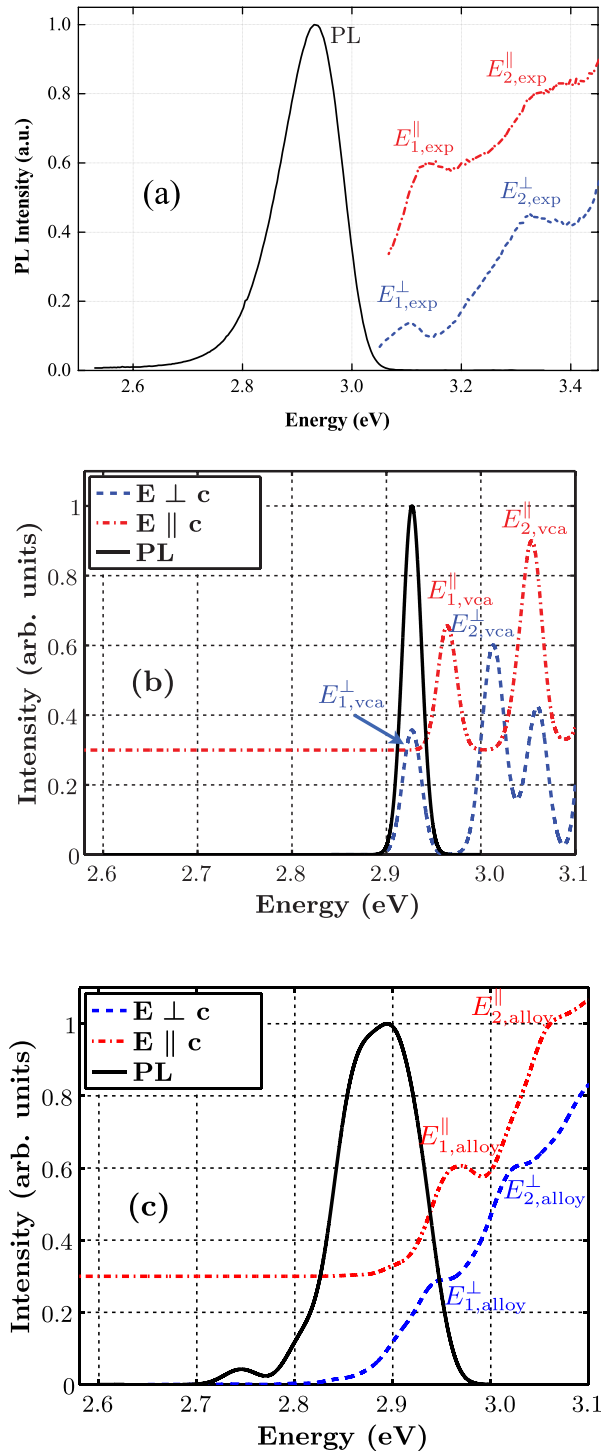


FIG. 1. (a) Low-temperature (10K) PL and PLE spectra for the *m*-plane InGaN/GaN QW sample. The PLE spectra are shown with the plane of polarization of the incident light perpendicular (blue dashed) or parallel (red dashed-dotted) to the crystal *c* axis. The PL spectrum is given by the black solid line. (b) Calculated PL and PLE within VCA. (c) Same as (b) but from the calculation including random alloy effects.

frame of reference to highlight the importance of random alloy fluctuations and related carrier localization effects. Thus, the purpose of the VCA is merely to establish general trends. To account for Coulomb effects, we have calculated 20 electron and 30 single-particle hole states and fed this into the CI scheme. To make these calculations feasible, especially since we have to include even more states in the fully atomistic calculation, we use a diagonal approximation

in the CI.²⁰ Since we are mainly interested in energetic shifts and exciton localization effects, this approximation should be sufficient. Results of the VCA calculations are depicted in Fig. 1(b). Similar to the experimental results, the unpolarized PL data are shown in black, while the (blue) dashed line gives the PLE data for $\mathbf{E} \perp \mathbf{c}$. The (red) dashed-dotted line corresponds to $\mathbf{E} \parallel \mathbf{c}$. The discrete transitions have been broadened by a Lorentzian with a broadening parameter of 10 meV. The chosen parameter is small enough not to affect the width of the final spectrum, but large enough for the spectrum to be relatively smooth when alloy effects are included on an atomistic level. When comparing theoretical and experimental data, we find several similarities and differences. The most striking difference between VCA and experiment is that in VCA the PL peak and the first excitonic transition in the PLE, $E_{1,vca}^+$, are at the same energetic position. This is exactly what one would expect from a continuum-like calculation since it completely neglects localization effects. However, the VCA captures several features of the PLE spectrum. For instance, the transition $E_{1,vca}^+$ lies energetically below the $E_{1,vca}^{\parallel}$ transition. This behavior is consistent with the experimental data (cf. Fig. 1(a)). The calculated splitting $\Delta E_{1,vca}^{\pm} = 37$ meV is in good agreement with the experimental value of $\Delta E_{1,exp}^{\pm} \approx 35$ meV. When looking at our VCA results, we find also a second set of these two peaks at the high energy side of our spectrum ($E_{2,vca}^+$ and $E_{2,vca}^{\parallel}$), which are related to excited electron and hole state transitions. A similar structure is visible in the experimental spectra ($E_{2,exp}^+$ and $E_{2,exp}^{\parallel}$ in Fig. 1(a)). Overall, the VCA reflects the main features of the measured PLE spectrum while it fails completely to describe the SS.

We have performed the same calculation now for a random distribution of In atoms in the QW by means of our atomistic TB theory. To achieve a realistic description of different microscopic configurations in the system, the calculations have been repeated 75 times for a fixed average In content of 17%. In the CI calculation, we have included 20 electron and over 100 hole single-particle states. Figure 1(c) shows the averaged results. The black solid line depicts the unpolarized PL spectrum. The low energy PL peak at 2.73 eV arises from a small number of exceptionally strongly localized states; more configurations would be required to reliably treat the importance of such states; thus, they are excluded from determining the SS. The PLE results are given by the (blue) dashed and (red) dashed-dotted line for $\mathbf{E} \perp \mathbf{c}$ and $\mathbf{E} \parallel \mathbf{c}$, respectively. When taking localized states due to random alloy fluctuations into account, we find a clear energetic separation between the PL and the first exciton peak in the PLE spectrum, denoted in the atomistic calculation by $E_{1,alloy}^+$. The calculated SS is $\Delta E_{alloy}^{Stokes} \approx 55$ meV. Even though it is smaller than the experimental value $\Delta E_{exp}^{Stokes} \approx 180$ meV, our calculations provide clear evidence that random alloy fluctuation effects can significantly modify the DOS and contribute to the SS. Furthermore, in comparison to the VCA, the random alloy fluctuations lead to a significant broadening of both the PL and PLE spectrum. The calculated FWHM of the PL is approximately 101 meV and is in good agreement with the experimentally extracted value of 134 meV. The calculated splitting between $E_{1,alloy}^+$ and $E_{1,alloy}^{\parallel}$ is $\Delta E_{1,alloy}^{\pm} \approx 23$ meV, similar to the experimental

value of $\Delta E_{1,\text{vca}}^{\perp,\parallel} \approx 35$ meV. Also, the polarization properties of the first two excitonic transitions $E_{1,\text{alloy}}^{\perp}$ and $E_{1,\text{alloy}}^{\parallel}$ are the same as in the VCA, Fig. 1(b), and consistent with the experiment, Fig. 1(a). However, when including random alloy fluctuations in the calculations, the peaks are significantly broadened, again similar to the experiment. The broadening arises because, due to the presence of random alloy affects, each microscopic configuration gives a slightly different transition energy. Consistent with the experiment, we find a second set of transitions $E_{2,\text{alloy}}^{\perp}$ and $E_{2,\text{alloy}}^{\parallel}$ on the high energy side of the PLE spectrum, which again originate from transitions between excited electron and hole states. The splitting between these two features, $\Delta E_{2,\text{alloy}}^{\perp,\parallel} \approx 40$ meV, is in good agreement with the VCA result.

Obviously, there are several differences between theory and experiment, likely due to a combination of several factors. First, the calculated SS is much smaller than the measured one. Since this quantity should depend strongly on the modification of the DOS due to the presence of localized states, the microstructure of the alloy plays a central role. As discussed above, deviations from a random In distribution, as assumed in the calculations, cannot be ruled out from our APT data. Since random alloy fluctuations lead to a significant SS, “clustering” effects in the alloy, as reported for α -plane QWs,²¹ should notably affect the DOS of localized states. Second, whilst both the In content and well width used in the calculations are within the experimentally measured ranges, deviations of the selected values from the true values within the experimental errors could affect the results. If the In content were larger, localization effects would become more pronounced,¹⁸ whilst a smaller well width would lead to a larger band gap and consequently to a later onset of the calculated excitonic transitions in the PLE spectrum. It is beyond the scope of the present study to analyze in detail the impact of these factors or of uncertainties related to material parameters such as band offsets, band offset ratios, or effective masses used in the calculations. The aim of this study is to establish general trends and highlight by explicit calculation the importance of the random alloy fluctuations on emission and absorption features in non-polar InGaN QWs.

In summary, we have presented a combined theoretical and experimental analysis of the emission and absorption features of m -plane InGaN/GaN QWs. The measured PL and PLE spectra have been compared with VCA and atomistic TB calculations. The VCA does not produce a SS since it neglects the effect of alloy disorder, but it reproduces the main features of the PLE spectrum, e.g., the splitting of the exciton states. These features are also reproduced by the fully atomistic treatment. Moreover, a discernible SS is observed when including random alloy fluctuations. Thus,

we demonstrate explicitly the importance of carrier localization due to random alloy fluctuations in determining the optical properties, not just PL spectra, in m -plane InGaN QWs.

This work was supported by Science Foundation Ireland (Project No. 13/SIRG/2210) and the United Kingdom Engineering and Physical Sciences Research Council (Grant Agreement Nos. EPJ001627\1 and EPJ003603\1). S.S. acknowledges computing resources provided by the SFI/HEA Irish Centre for High-End Computing. R.A.O. and F.T. acknowledge the support of the European Research Council under the European Community’s 7th Framework Programme (FP7/2007–2013)/ERC Grant Agreement No. 279361 (MACONS).

¹S. Nakamura, *Science* **281**, 956 (1998).

²M. Auf der Maur, A. Pecchia, G. Penazzi, W. Rodrigues, and A. Di Carlo, *Phys. Rev. Lett.* **116**, 027401 (2016).

³J. Piprek, *Appl. Phys. Lett.* **107**, 031101 (2015).

⁴S. Nakamura, T. Mukai, and M. Senoh, *Appl. Phys. Lett.* **64**, 1687 (1994).

⁵P. Dawson, S. Schulz, R. A. Oliver, M. J. Kappers, and C. J. Humphreys, *J. Appl. Phys.* **119**, 181505 (2016).

⁶S. F. Chichibu, A. Uedono, T. Onuma, B. A. Haskell, A. Chakraborty, T. Koyama, P. T. Fini, S. Keller, S. P. DenBaars, J. S. Speck *et al.*, *Nat. Mater.* **5**, 810 (2006).

⁷Y.-H. Cho, G. H. Gainer, A. J. Fischer, J. J. Song, S. Keller, U. K. Mishra, and S. P. DenBaars, *Appl. Phys. Lett.* **73**, 1370 (1998).

⁸S. Hammersley, D. Watson-Parris, P. Dawson, M. J. Godfrey, T. J. Badcock, M. J. Kappers, C. McAleese, R. A. Oliver, and C. J. Humphreys, *J. Appl. Phys.* **111**, 083512 (2012).

⁹C. Delalande, M. H. Meynadier, and M. Voos, *Phys. Rev. B* **31**, 2497 (1985).

¹⁰G. P. Kothiyal and P. Bhattacharya, *J. Appl. Phys.* **63**, 2760 (1988).

¹¹S. F. Chichibu, A. C. Abare, M. P. Mack, M. S. Minsky, T. Deguchi, D. Cohen, P. Kozodoy, S. B. Fleischer, S. Keller, J. S. Speck *et al.*, *Mater. Sci. Eng. B* **59**, 298 (1999).

¹²J. Hader, J. V. Moloney, and S. W. Koch, *Appl. Phys. Lett.* **89**, 171120 (2006).

¹³P. Waltereit, O. Brandt, A. Trampert, H. T. Grahn, J. Menniger, M. Ramsteiner, and K. H. Ploog, *Nature* **406**, 865 (2000).

¹⁴S. Schulz, D. P. Tanner, E. P. O’Reilly, M. A. Caro, T. L. Martin, P. A. J. Bagot, M. P. Moody, F. Tang, J. T. Griffiths, F. Oehler *et al.*, *Phys. Rev. B* **92**, 235419 (2015).

¹⁵S. Schulz, T. J. Badcock, M. A. Moram, P. Dawson, M. J. Kappers, C. J. Humphreys, and E. P. O’Reilly, *Phys. Rev. B* **82**, 125318 (2010).

¹⁶D. Watson-Parris, M. J. Godfrey, P. Dawson, R. A. Oliver, M. J. Galtrey, M. J. Kappers, and C. J. Humphreys, *Phys. Rev. B* **83**, 115321 (2011).

¹⁷S. Schulz, M. A. Caro, C. Coughlan, and E. P. O’Reilly, *Phys. Rev. B* **91**, 035439 (2015).

¹⁸D. P. Tanner, M. A. Caro, E. P. O’Reilly, and S. Schulz, *RSC Adv.* **6**, 64513 (2016).

¹⁹M. A. Caro, S. Schulz, and E. P. O’Reilly, *Phys. Rev. B* **88**, 214103 (2013).

²⁰N. Baer, S. Schulz, P. Gartner, S. Schumacher, G. Czycholl, and F. Jahnke, *Phys. Rev. B* **76**, 075310 (2007).

²¹F. Tang, T. Zhu, F. Oehler, W. Y. Fu, J. T. Griffiths, F. C.-P. Massabuau, M. J. Kappers, T. L. Martin, P. A. J. Bagot, M. P. Moody *et al.*, *Appl. Phys. Lett.* **106**, 072104 (2015).